Predicting the statistics of wave transport through chaotic cavities by the random coupling model: A review and recent progress

Gabriele Gradoni, Jen-Hao Yeh, Bo Xiao, Thomas M. Antonsen, Steven M. Anlage *, Edward Ott

Institute for Research in Electronics and Applied Physics, University of Maryland, College Park, MD-20742, USA
Department of Physics, University of Maryland, College Park, MD-20742, USA
Department of Electrical and Computer Engineering, University of Maryland, College Park, MD-20742, USA

HIGHLIGHTS

- Develop a quantitative model of complex wave scattering systems.
- The model applies to electromagnetics, vibro-acoustics, and quantum mechanics.
- Theoretical concepts are supported with experimental and numerical results.
- New applications to systems with large apertures and to interconnected systems.
- Direct connection made to the statistical energy approach in vibro-acoustics.

ARTICLE INFO

ABSTRACT

In this review, a model (the random coupling model) that gives a statistical description of the coupling of radiation into and out of large enclosures through localized and/or distributed ports is presented. The random coupling model combines both deterministic and statistical phenomena. The model makes use of wave chaos theory to extend the classical modal description of the cavity fields in the presence of boundaries that lead to chaotic ray trajectories. The model is based on a clear separation between the universal statistical behavior of the closed chaotic system, and the deterministic coupling port characteristics. Moreover, the ability of the random coupling model to describe interconnected cavities, aperture coupling, and the effects of short ray trajectories is discussed. A relation between the random coupling model and other formulations adopted in acoustics, optics, and statistical electromagnetics, is examined. In particular, a rigorous analogy of the random coupling model with the Statistical Energy Analysis used in acoustics is presented.

© 2014 Elsevier B.V. All rights reserved.

1. Introduction

Increasingly complex scenarios in electronics and telecommunications make the detail of structures and circuitry more and more difficult to model. In addition, often in optics, electronics, and acoustics, the need for higher bit-rates pushes wave sources to emit at very short wavelengths compared to the characteristics size of the excited system. In this regime, the scattering process can be very sensitive to details. The complex boundary shape of an enclosure can lead to the phenomenon

---

of ray chaos in which a ray trajectory inside the enclosure shows strong sensitivity to initial conditions. From experimental observations, it is known that this results in a very high variability of wave properties of the system. A statistical approach to understanding the short-wavelength properties of the system then becomes appropriate. Specifically, one can ask what the statistics of quantities of interest are relative to a suitable random choice of the system, and this is the goal of the RCM. Other statistical approaches have already been used to study reverberation chambers [1,2] and wireless propagation channels. The RCM is based on the flexibility of the random matrix theory (RMT).

1.1. Random matrix theory background

As with other formulations involving complex wave systems of different physical nature, the RCM is based on features of RMT.

Beginning in 1982 there was rapid development in the application of RMT to both quantum and classical wave systems. The first use of RMT was devoted to reproducing the spacing distribution of energy levels in compound nuclei. Those distributions are reproduced from eigenvalues of large random matrices belonging to two statistical ensembles: the Gaussian orthogonal ensemble (GOE), and the Gaussian unitary ensemble (GUE). In both cases, all the matrix elements are zero-mean Gaussian random variables. In the GOE all the diagonal element distributions have the same width, while all the off-diagonal element distributions have widths that are half that of the diagonal elements. The matrices are constrained to be symmetric, but otherwise the elements are statistically independent. The GOE case is intended to model wave systems that have time reversal symmetry (TRS). In the GUE the matrices are constrained to be Hermitian. In this case the off-diagonal elements are complex and the distributions of their real and imaginary parts are independent and Gaussian and the width of these Gaussians is again one half the width of the real diagonal elements. The GUE case is intended to model systems for which time reversal symmetry is broken (TRSB). This case will apply in electromagnetics if a nonreciprocal element such as a magnetized ferrite or a cold magnetized plasma is added to the system. In this paper, eigenvalues of a random matrix of the Gaussian Orthogonal Ensemble (GOE) with Gaussian distributed elements have been used since the time-reversal invariance is assumed to hold.

More recently, in nuclear theory, the so called *R*-matrix theory has been developed as a statistical model for the interaction of compound nuclei with external particles through discrete reaction channels [3,4]. The R-matrix description was later applied to resonant electromagnetic cavities [5]. Other fields of investigation of RMT concern Rydberg levels of the hydrogen atom in a strong magnetic field, elastomechanical eigenfrequencies of irregularly shaped quartz blocks, as well as fluctuations of conduction through mesoscopic wires in a magnetic field [6,7,4]. In quantum mechanics, studies of RMT applied to quantum transport gathered profound interest [8,9]. Besides nuclear theory, mesoscopics, and quantum mechanics, several applications of RMT can be found in acoustics and vibration systems [10–12]. The pure statistical perspective of physical systems adopted in these fields is even older and originates from thermodynamics. Interestingly, this perspective led spontaneously to the use of random matrices for modeling transmission of vibrational energy. Specifically, a model in acoustics that is close to those in electromagnetics can be found in the so-called statistical energy analysis (SEA) [13]. This method is currently used as a key strategy in developing numerical tools for analysis of vibrational energy in complex mechanical systems [14]. Furthermore, semiclassical wave functions and RMT have been widely used to understand and model wave scattering in complex systems. In particular, the effective Hamiltonian approach was developed to model open electromagnetic cavities with a random scattering matrix [15,16].

However, only a small number of experiments on wave-chaotic scattering and eigenfrequencies of electromagnetic cavities existed. The first studies of irregularly shaped microwave cavities [17–20] paved the way to electromagnetic wave-chaotic scattering research. Microwave cavities with irregular shapes (having ray trajectories evolved by a chaotic map) provided a simple and effective physical framework for the study of wave-chaos, where not only the magnitude, but also the phase of scattering coefficients, can be directly measured from experiments.

Both the presence of localized ports [21] and slits [22] have been investigated experimentally for wave chaotic billiards showing interesting physical phenomena such as avoided level-crossing, and resonance trapping. Furthermore, absorption mechanisms have been accounted for by several authors [23,5,24–27].

1.2. Random coupling model novelty

The RCM addresses the problem of statistically modeling the wave behavior of large irregular cavities connected to an external environment by one or more ports. The applicability of the RMT to the solution of simple wave equations in bounded regions where the corresponding ray trajectories are chaotic was originally explored by [28]. From a practical point of view, it is hard to avoid the ray chaos regime, even in nominally regular enclosures. The presence of objects in the interior region of the cavity, or simply the presence of antennas (ports, apertures) makes the cavity irregular: this can be seen in the statistical properties of the cavity spectrum [29]. The signature of wave chaos can be appreciated in the port impedance, which becomes a strong function of frequency and details of cavity shape, as well as of internal configuration and components [30].

The main goal in formulating the RCM was to connect the behavior predicted by the RMT developed for the case of isolated wave chaotic systems, e.g., closed cavities, to the study of the behavior of such a system when it is connected to other systems

through deterministic wave propagation ports, and to investigate the resulting input/output system characteristics. This was done earlier in the quantum mechanical context, for example, by [31–33,8,6,34–38]. The RCM was developed for resonators with spatially localized ports [39]. In 2006, studies were published for both the single port [40], and the multiple port [41] cases.

The RCM attacks this problem from the point of view of cavity impedance (admittance), in which the universal fluctuations of fields within the cavity is joined to the specific radiation characteristics of deterministic ports, whose geometry is presumed to be known *a priori*.

In the past, statistical electromagnetics (SEM) introduced the use of statistics and stochastic analysis to model complex electromagnetic systems [42]. Cavities and resonators constitute a natural and fertile terrain for SEM to be developed and applied. A number of models have been proposed to explain and predict fluctuations inside cavities (see for example [1]). The RCM improves on those phenomenological theories by describing random fluctuations through statistical ensemble theories [43]. In contrast to SEM, the RCM builds on the exact model of impedance and admittance matrices as derived from Maxwell's equations. In contrast to the scattering matrix employed in the effective Hamiltonian approach, the admittance/impedance matrix employed in the RCM is defined as an "open-circuit" transfer function of the system.

2. Overview of the random coupling model

Here we give a brief overview of the key conceptual features of the RCM before getting into the details in Section 3.

The derivation of the RCM exploits both the Wigner surmise [44] and the Berry hypothesis [45]. If the dimensions of the cavity are much greater than the excitation wavelength, the semiclassical regime can be invoked. Irregular boundaries create highly disordered mode topologies. Therefore, the mode amplitude is locally modeled as an isotropic random superposition of plane waves (the Berry hypothesis). The motivation of this hypothesis is that the orbits of rays in a fully chaotic system visit all regions of phase space ergodically. In particular, if some time along a long orbit is randomly chosen, the probability density of the orbit direction is uniform in 0 to 2π in a 2D cavity, while it is uniform in 0 to 4π (solid angle) in a 3D cavity.

From Wigner's hypothesis it follows that the mode wavenumbers for a complicated (in our case chaotic) system have the same statistics as the eigenvalues predicted by RMT, where the choice of a suitable statistical ensemble type depends on the time-reversal symmetry property of the modeled system.

Therefore, the wave chaos inside the cavity is then expressed as a universal (i.e., system independent) superposition of modes defined by physically-based statistical prescriptions. The presence of ports connected with the external environment results in "dressing" this superposition with the radiation impedance matrix Z^{rad} of port terminals. In electromagnetics, the ratio of the electromotive voltage over the excitation current on terminals defines the impedance. In acoustics, the impedance is defined by the ratio of the acoustic pressure, analogous to the electromotive voltage, and the acoustic volume flow, analogous to the excitation current in electromagnetic systems. The electromagnetic impedance indicates how much electromotive force is generated as a reaction to the injection of an external current flow of charges. The acoustic impedance indicates how much sound pressure is generated by a given air vibration.

In the case of a cavity with a single port the cavity impedance Z^{cav} can be expressed as

$$Z^{cav} = i\Im\left\{Z^{rad}\right\} + \Re\left\{Z^{rad}\right\}\xi, \tag{1}$$

where Z^{rad} is the complex port radiation impedance that will be defined later in the paper, and $\Im\{\cdot\}$ and $\Re\{\cdot\}$ denote imaginary and real parts. In (1), ξ is a unitless random variable given by a modal superposition, discussed in detail in Section 3. Thus, the statistics of Z^{cav} are determined by the statistics of the random variable ξ and by the nonstatistical quantity Z^{rad}. The random variable is universal in the sense that it depends only on a scalar parameter α. This parameter includes cavity losses and modal structure through an average (modal) quality factor as well as the mean spacing between nearest neighbor eigenmodes [44], and on no other cavity details. It is important to point out that the loss factor does not include the effect of ports on broadening the resonances. In particular, the average quality factor that we use is defined as an ensemble average over the isolated cavity resonances. For large mode overlapping (high α) [46,1], we can borrow the concept of compound quality factor used in well-overmoded reverberation chambers [47]. We believe that a representation in terms of α can be applied to any overlapping regime provided the number of participating cavity modes is very high, the cavity spectrum is consistent with the RMT description, and the ports are far from metallic boundaries [30, see page 768].

The RCM introduces and incorporates system-specific characteristics in a single and compact form. It will be shown how deviations from pure wave chaos in the enclosure can be included in the RCM by considering short-ray orbits [48,49]. The RCM impedance expression (1) is preserved and the non-universal term is augmented with information about "non-chaotic" short ray orbits [50]. The model has been verified experimentally for cavities with either one or two ports [51–59,30].

Recently, the RCM has been further developed for three dimensional cavities with distributed ports (e.g., complicated antennas) in the same form as Eq. (1) [60]. The presence of apertures calls for a different modeling attack, leading to the same form of the RCM for the cavity admittance. The problem of external radiation coupling to the cavity through an aperture has been solved [61–63].

In realistic physical scenarios one may employ different kinds of port coupling to a closed electromagnetic environment (EME). Imagine a situation involving compartments of ships/aircraft/automobiles/trains: there could be present very localized terminals belonging to circuitry located inside bays, as well as very large windows and ports. It is thus quite useful

to formulate a "hybrid" RCM involving both port terminals and electrically wide apertures, and to consider interconnected cavities.

The structure of Eq. (1), in which the radiation impedance multiplies and offsets the universal fluctuations, is particularly simple. The radiation impedance is known from experimental characterization of the port, or from solution of Maxwell's equations in free-space. Such a simple form for the "dressed" quantity does not exist for the scattering matrix. Furthermore, the impedance (admittance) approach can be easily generalized to include other deterministic corrections, such as short orbits [50,57] and modeling of mixed systems [64].

In the following sections, the general formulation of the RCM for ports and apertures is reviewed. Then, the predictions of probability distribution functions of desired input/output parameters (e.g., impedances, admittances or scattering parameters) obtained for single-mode ports by Monte Carlo computation of the RCM, and their experimental confirmation by measurements on actual systems are recalled. Finally, an application of the model to a situation of practical interest is discussed: the modeling of linear chains of interconnected chaotic cavities [65].

3. Random coupling model details

3.1. The impedance description

The RCM is conveniently formulated in terms of an impedance or admittance matrix. The use of network theory for solving electromagnetic problems is widely accepted in engineering and physics [66]. This often leads to theoretical formulae that can be efficiently computed and compared with measurements. In particular, the use of *open-circuit* parameters such as impedances and admittances does not require any specific knowledge of the sources and detectors connected to the terminals where voltages and currents are supposed to exist. Imagine injecting an excitation *current* into a small antenna radiating inside an irregular cavity. The multiple reflections and scattering of rays off the metallic (lossy) walls establish a reaction to the current density flowing on the antenna surface. This creates an electromotive force that builds up the response *voltage* at the terminals of the antenna. In the case of a single port, the ratio of the reaction voltage over the excitation current defines the terminal impedance. In the specific case where the antenna radiating inside a cavity, the impedance is called the *cavity impedance* [40]. In the presence of multiple ports, the response effect of the excitation current on each antenna terminal can be easily separated by defining a cavity impedance matrix $\underline{\underline{Z}}^{cav}$ [40].

$$V_p = \sum_{p'} Z_{pp'}^{cav}(k_0) I_{p'}, \tag{2}$$

where p labels the ports of the system, I_p is the current applied to port p, V_p is the voltage appearing on port p, and k_0 is the free-space wavenumber of the port signals. To find $Z_{pp'}^{cav}$ in 3D cavities, a solution of the vector wave equation satisfying cavity boundary conditions is constructed. This is done through the usual procedure of expanding the cavity fields in a basis of electromagnetic and electrostatic eigenmodes. At this point, the prescriptions of the RCM based on wave chaos and random matrix theory are used. Firstly, the exact cavity spectrum is replaced with a spectrum of eigenvalues generated by a large random matrix of the appropriate symmetry (as discussed in Section 2). The mode amplitude (which is unknown) is replaced with a superposition of random plane-waves. The RCM prescriptions lead to a fluctuating impedance matrix $\underline{\underline{\xi}}$ having dimension $N_p \times N_p$, where N_p is the number of ports connected to the cavity, viz.,

$$\underline{\underline{Z}}^{cav} = i\Im\left\{\underline{\underline{Z}}^{rad}\right\} + \left[\Re\left\{\underline{\underline{Z}}^{rad}\right\}\right]^{1/2} \cdot \underline{\underline{\xi}} \cdot \left[\Re\left\{\underline{\underline{Z}}^{rad}\right\}\right]^{1/2}, \tag{3}$$

where $\underline{\underline{Z}}^{rad} = \underline{\underline{R}}^{rad} + i\Im\left(\underline{\underline{Z}}^{rad}\right)$ is in the simplest theory an $N_p \times N_p$ diagonal matrix whose elements are the complex radiation impedances of each port. Here, the radiation impedance provides the linear relation between voltages and currents at a port in the case in which waves are allowed to enter the enclosure through the port but not return, as if they were absorbed in the enclosure or radiated to infinity. The universal random matrix $\underline{\underline{\xi}}$ naturally incorporates homogeneous cavity losses, and it is defined as

$$\underline{\underline{\xi}} = -\frac{i}{\pi} \sum_n \frac{\Phi_n \Phi_n^T}{\mathcal{K}_0^2 - \mathcal{K}_n^2 + i\alpha}, \tag{4}$$

where $\mathcal{K}_{(\cdot)}^2 = k_{(\cdot)}^2/\Delta k^2$, Δk^2 is the mean mode spacing, k_n are cavity mode wavenumbers, and α is the loss parameter defined below. Here, $\underline{\Phi}_n$ is a vector of uncorrelated, zero mean, unit width Gaussian random variables, representing (unitless) random coupling coefficients between port current profiles and cavity eigenmodes (this is where the Random Coupling Model gets its name), and k_n^2 are the eigenvalues of a matrix selected from the GOE [67], where the central eigenvalue is shifted to be close to $k_0^2 = \omega^2/c^2$, and ω is the frequency of excitation. In the case of a high number of overlapping modes, e.g., occurring in overmoded reverberation chambers [1], the eigenvalues have uniform distribution and are distributed as per Wigner's "semicircle law" (see [30, Appendix] and [67] for more details). Eigenvalues associated with participating modes are scaled so that the average spacing between eigenvalues near the central one is Δk^2, which is selected to match

the mean spacing of resonances of the enclosure in the frequency range of interest. The effect of wall losses, internal homogeneous losses and the cavity dimensions (volume), are embedded into a single dimensionless loss parameter

$$\alpha = \frac{k_0^2}{Q \Delta k^2},$$ (5)

appearing in (4), which is formally identical to the *inverse finesse parameter*, widely used in optical resonators to quantify the granularity of resonances over a frequency band of interest [68], and where the (average) cavity quality factor is defined as

$$Q = \omega \frac{E}{P_d},$$ (6)

with E, the average energy stored inside the cavity, and P_d, the total power dissipated throughout the cavity in the resonant mode. The loss parameter α ranges from 0 to infinity, and the greater α the higher the resonance overlapping over the considered bandwidth. As already pointed out, the single parameter description is accurate for a cavity whose spectrum is wave chaotic with high modal density. Further investigation is needed to verify the applicability of the RCM at low modal densities [69,70], e.g., undermoded operation of or proximity to metallic boundaries in electromagnetic reverberation chambers [71]. In the lossless case, $\underline{\underline{\xi}}$ has purely imaginary elements, and it is found to be an element of the Lorentzian ensemble [72]. In the high-loss case, $\underline{\underline{\xi}}$ has complex elements whose imaginary part tends to a zero mean Gaussian distribution, and whose real part distribution is asymmetric with average value 1 [40,41].

It is through the matrix $\underline{\underline{\xi}}$ that the propagation of waves in the enclosure from one port to another and back is modeled. Such a propagation is universally fluctuating with statistics regulated by a single parameter, α. The enclosure itself is modeled by (4), which accounts for the chaotic scattering taking place throughout the cavity. Rapid variations of impedance with frequency arise from the underlying ray-chaotic behavior. Similarly, in acoustics and vibrational systems, the acoustic impedance usually varies strongly when the frequency is changed. The form (3) makes a perfect link with well-established deterministic theories. The RCM treats ports by means of a slowly-varying-in-frequency radiation impedance matrix. The novelty of the RCM resides in the definition of a 'random' impedance that is *dressed with deterministic features.*

3.2. Short-orbit corrections

Experiments involving ray-chaotic cavities often rely on the variation of boundary configuration to create numerous statistically independent realizations of the system and to compile statistics [46,73–75]. From a wave chaotic perspective, it is noted that the port–port interaction introduces deterministic field components that can remain fixed throughout the ensemble (such as wall proximity on scattering objects inside the enclosure). This kind of "imperfection" has been widely investigated in quantum chaos [76,77]. Therefore, relevant ray trajectories, which remain unchanged in many or all realizations of the ensemble, may exist and represent another system-specific feature. In practical mode-stirred reverberation chambers, it is expected that perfect mixing leads to a zero mean complex field over a number of cavity realizations dependent on the working frequency range [78]. However, an offset in the scatter plot of the measured field is often experienced. Numerical and experimental observations of those "imperfect" reverberation fields are reported in [79–81]. This phenomenon is believed to be related to "short orbits", defined as trajectories that leave a port and soon return to it, or another port, instead of ergodically sampling the system. In other words, a short-orbit can be defined as a trajectory evolving for a time less than or equal to the Ehrenfest time (discussed in detail below). Before this time scale the electromagnetic waves generated by the ports are well described as a classical coherent ray. Beyond this time scale, the classical chaos mixes the ray trajectories destroying the ray description for the waves.

It is imagined that each ray leaves from a port p at $\mathbf{r}_i$ with a certain $\mathbf{k}_i$ vector and it arrives at port p' at final position $\mathbf{r}_f$ with a wave vector $\mathbf{k}_f$. It is further assumed that the ports are separated from the wall much more than a wavelength. [50,56,57] extended the RCM to take account of such ray trajectories. The theory exactly treats short-orbits by considering the port configuration with respect to cavity boundaries. This has been done by solving the surface integral equation (SIE) related to the general boundary-value problem. In particular, the kernel of the SIE for the port impedance matrix has been expressed in terms of a semiclassical transfer operator, which traces all the possible ray trajectories involved in the specific port configuration. This philosophy is similar to that of the Poisson kernel [82,15], where those contributions arising from non-random system-specific part are included in the scattering matrix elements by following an information theoretic approach. The impedance form of the RCM results in an expression where the system-specific aspect of the short-orbits is captured by the average impedance.

Mathematically, it is found by a semiclassical theory of orbits [50]

$$\underline{\underline{Z}}^{cav} = i\Im\left\{\underline{\underline{Z}}^{rad}\right\} + \underline{\underline{v}}^\dagger \cdot \left[\underline{\underline{1}} + \underline{\underline{T}}\right] \cdot \left[\underline{\underline{1}} - \underline{\underline{T}}\right]^{-1} \cdot \underline{\underline{v}},$$ (7)

where $\underline{\underline{v}}$ is an $N \times M$ matrix defined by the boundary integral equations [50, Eqs. (12)], and it is normalized by [50, Eq. (36)]

$$\underline{\underline{v}}^\dagger \cdot \underline{\underline{v}} = \Re\left\{\underline{\underline{Z}}^{rad}\right\},$$ (8)

and where $\underline{\underline{T}}$ is the Bogomolny *transfer matrix*, having dimensions $M \times M$, with the finite dimension M defined in [83], and whose elements can be expressed as, in the electromagnetic case [84]

$$T_{if}\left(q_i, q_f, \mathbf{k}\right) = \frac{-i}{4} \sqrt{D_{\mathbf{r}_i, \mathbf{r}_f}} \, e^{iS\left(\mathbf{r}_i, \mathbf{r}_f, \mathbf{k}\right) - i\frac{\pi}{4}} \sqrt{\frac{\cos \theta_f}{\cos \theta_i}}, \tag{9}$$

where θ_i (θ_f) is the angle between the initial (final) wave vector and the surface at the position it leaves (hits), $S\left(\mathbf{r}_i, \mathbf{r}_f, \mathbf{k}\right)$ is the classical action-angle variable along the direct trajectory from $\mathbf{r}_i$ to $\mathbf{r}_f$, defined as the integral of the linear momentum ($\mathbf{k}$ for electromagnetic waves) over the ray path bouncing off of dispersive walls and $\sqrt{D_{\mathbf{r}_i, \mathbf{r}_f}}$ is the stability of the orbit from $\mathbf{r}_i$ to $\mathbf{r}_f$ (monodromy) that physically represents a geometrical factor of the trajectory taking account of the spreading of the ray tube along its path. The stability is mathematically defined as [50, Eq. (20)]

$$D_{\mathbf{r}_i, \mathbf{r}_f} = \frac{2}{\pi k^2} \left| \frac{\partial^2 S\left(\mathbf{r}_i, \mathbf{r}_f, \mathbf{k}\right)}{\partial \mathbf{r}_{i,\perp} \, \partial \mathbf{r}_{j,\perp}} \right|, \tag{10}$$

where the derivative with respect to $\mathbf{r}_{j,\perp}$ represent the gradient of $\mathbf{r}_j$ dotted in to the unit vector perpendicular to $\mathbf{k}_{(\cdot)}$. Even though the short-orbit correction has been derived for 2D electromagnetic billiards, an extension to the 3D case can be done in principle.

Ultimately, the correction introduced by the presence of short-orbits can be expressed as an RCM average impedance as

$$\underline{\underline{Z}}^{avg} = \left\langle \underline{\underline{Z}}^{cav} \right\rangle = i\Im \left\{ \underline{\underline{Z}}^{rad} \right\} + \left[\Re \left\{ \underline{\underline{Z}}^{rad} \right\} \right]^{1/2} \cdot \underline{\underline{z}} \cdot \left[\Re \left\{ \underline{\underline{Z}}^{rad} \right\} \right]^{1/2}, \tag{11}$$

where the elements of $\underline{\underline{z}}$ are expressed as

$$z_{n,m} = \sum_{b(n,m)} -p_b \sqrt{D_b} \exp\left[-\left(i \left| \mathbf{k} \right| + k' \right) L_b - i \left| \mathbf{k} \right| L_{port} - i\beta_b\pi \right], \tag{12}$$

with $b(n, m)$ an index over all classical trajectories which leave the nth port, bounce β_b times, and return to the mth port, L_b is the length of the trajectory b, $k' = k/(2Q)$ is the effective attenuation parameter taking account of loss through the average quality factor Q, and L_{port} is the port-dependent constant length between the nth and mth port. In (12), p_b is the survival probability of the trajectory in the ensemble, and D_b is the stability defined in (10) now evaluated along the trajectory b. The stability D_b is a function of the length of each segment of the trajectory, the angle of incidence of each bounce, and the radius of curvature of each wall encountered in that trajectory. The detailed generation of short-orbit trajectories, and the numerical calculation of both p_b and D_b, depending on the geometry of the cavity boundary, is detailed in [57]. As with Eq. (3), the RCM in the presence of short-orbits can be expressed as a compact impedance matrix where the system-specific characteristics of ports are clearly separated from the universal fluctuation matrix of the cavity, viz.,

$$\underline{\underline{Z}}^{cav} = i\Im \left\{ \underline{\underline{Z}}^{avg} \right\} + \left[\Re \left\{ \underline{\underline{Z}}^{avg} \right\} \right]^{1/2} \cdot \underline{\underline{\xi}} \cdot \left[\Re \left\{ \underline{\underline{Z}}^{avg} \right\} \right]^{1/2}, \tag{13}$$

where $\underline{\underline{Z}}^{avg}$ is defined in (11).

The application of this theory to reverberation chambers could pave the way to understand and use the *single-frequency* regime, where comparison of experimental and theoretical statistics often exhibits strong deviations from asymptotic distributions [79].

Researchers have examined short orbits in cases where the system and the ports can be treated in the semiclassical approximation [76] or considered the effect on eigenfunction correlations due to short orbits associated with nearby walls [85]. Theoretical results have been previously obtained that acknowledge the effects of short-orbits in the context of quantum graphs [86]. The RCM for microwave cavities has been confirmed by experiments [57]. Moreover, experiments in a 2D microwave cavity have extracted a measure of the microwave power that is emitted at a certain point in the cavity and returns to the same point after following all possible classical trajectories of a given length [87]. None of this prior work developed a general first-principles deterministic approach to experimentally analyze the effect of short ray trajectories. The effect of short trajectories in two-port wave-chaotic cavities has been demonstrated [56,57]. The results of the short-orbit correction can be generalized to distributed ports and apertures by similar procedures. For apertures, it is interesting to think about the proximity of a dielectric/metallic object that is immersed in the wave-chaotic field. This physical situation has been investigated by Harrington in the case of regular cavities, where the aperture-object resonance was predicted by method of moments [88].

3.3. Aperture radiation of cavities

Besides localized ports, the RCM can also include a description of apertures, a situation depicted in Fig. 1: the scheme represent an open cavity, where there is an electrically wide aperture A, and an electrically small port P. The port can be
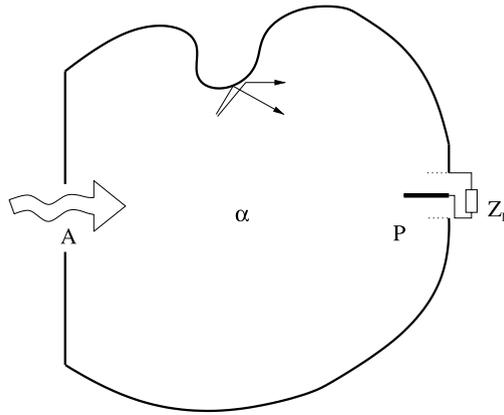
Fig. 1. Wave chaotic enclosure (described by loss parameter α) with both one aperture (A) and one port (P). The port is terminated with a load impedance Z_L.

thought as a monopole antenna entering an electrically small opening in a cavity wall, or a central conductor of a coaxial cable with the shield connected to the cavity wall. The port is terminated with a load Z_L.

Ongoing research is focusing on the extension to very large and irregular apertures, as well as to very small apertures, where singular fields strongly affect their (system specific) radiation [89]. The aperture excitation of an irregular enclosure is indeed a rather new theoretical problem to investigate. Interestingly, such a theory develops well on the existing literature on *cavity backed apertures*, and it links deterministic theories with statistical theories on reverberation chambers. The work of Harrington on cavities showed that boundary-value problems involving apertures are conveniently described in terms of the admittance matrix [90], and they can be solved numerically through the method of moments. On the other hand, it is known that when the cavity is strongly perturbed by irregular objects and/or boundaries, modes change their topology and spectrum completely, e.g., mode stirred enclosures/chambers [91], and the fields become amenable to statistical description [1]. Also in the presence of apertures, thanks to the RCM perspective of separating system-specific from universal characteristics, those two apparently distinct approaches can be unified through wave chaos theory. Similar to a port, the aperture geometry is fully included in the model through the radiation admittance matrix. The procedure to be followed is practically the same as that used to arrive at Eq. (3). A detailed mathematical derivation is described in [63], and is briefly recapitulated below.

The aperture has been treated as an opening in a zero thickness metallic plane, and the analysis started by expanding the aperture (tangential) field distribution in a basis of modes. The linear relation between magnetic field mode amplitude and electric field mode amplitude is expressed in terms of an admittance $Y_{ss'}^{(\cdot)}(k_0)$, where s and s' indicate the aperture mode index, and k_0 is the wavenumber of the external radiation impinging onto the aperture. In particular, $Y_{ss'}^{(\cdot)} = Y_{ss'}^{(rad)}$ or $Y_{ss'}^{(\cdot)} = Y_{ss'}^{(cav)}$ depending on whether the aperture radiates into free space or into a cavity. In particular, in the presence of the cavity, the boundary-value problem is solved by expanding the cavity fields in modes, and then by applying the RCM prescriptions for the properties of these modes. In this case, the RCM formulation leads to a specific relation between free-space admittance $Y_{ss'}^{(rad)}$ and cavity admittance $Y_{ss'}^{(cav)}$, viz.,

$$\underline{\underline{Y}}^{cav} = i\Im\left\{\underline{\underline{Y}}^{rad}\right\} + \left[\Re\left\{\underline{\underline{Y}}^{rad}\right\}\right]^{1/2} \cdot \underline{\underline{\xi}} \cdot \left[\Re\left\{\underline{\underline{Y}}^{rad}\right\}\right]^{1/2}, \tag{14}$$

where the matrix $\underline{\underline{\xi}}$ is the same as defined in (4), and the elements of $\underline{\underline{Y}}^{rad}$ are defined by [63]. Note that this has the same form as Eq. (3) for the cavity impedance in the case of discrete ports.

Eq. (14) is an equivalent network representation similar to that used in [90] to solve deterministic aperture problems. The fact that the system is open is accounted for by the presence of a magnetostatic admittance besides an electromagnetic admittance [92]. It is worth noticing that the rigorous derivation of the RCM for both the impedance and the admittance matrix yields the same universal fluctuation matrix $\underline{\underline{\xi}}$. In the lossless case, $\underline{\underline{\xi}}$ is also Hermitian. In the RCM, the system is described from the ports/apertures perspective, which requires an extension of the conventional RMT for generating eigenmodes of the open cavities.

3.4. Coupling with external radiation

In practical electromagnetic systems, an aperture can be fed by a wave-guide with the same transverse sectional shape, or it can be exposed to free-space external radiation. In both cases the expansions of the aperture tangential field in a basis of modes can be preserved. It is thus instructive to analyze the typical scenario depicted in Fig. 2 of an oblique plane-wave with wave vector $\mathbf{k}^{inc}$ and polarization of magnetic field $\mathbf{h}^{inc}$ (perpendicular to $\mathbf{k}^{inc}$) exciting the aperture. In [90], this analysis
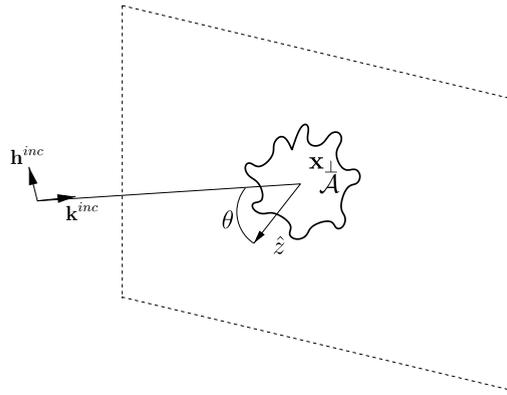
Fig. 2. Geometry of an aperture of arbitrary shape illuminated by an external plane-wave. The dashed rectangle represents one wall of the enclosure, and is assumed to be very large compared to the aperture area $\mathcal{A}$, $\mathbf{x}_\perp$ indicates the spatial location within the aperture area, $\hat{z}$ is the outward normal to the aperture plane, and θ is the angle between $\hat{z}$ and $\mathbf{k}^{inc}$ of the incident radiation.

has been performed by continuity of tangential magnetic field at the aperture plane, that leads to the equivalent network equation by projecting the two magnetic field expressions on the basis of aperture modes, and equating the amplitudes [61–63]

$$\left(\underline{\underline{Y}}^{cav} + \underline{\underline{Y}}^{rad} \right) \cdot \underline{V} = 2\underline{I}^{inc}, \tag{15}$$

where $\underline{V}$ is a *vector containing the projection of the incident field on to the basis of modes*, $I_s^{inc} = -\hat{n} \cdot \tilde{\mathbf{e}}_s \left(-\mathbf{k}_\perp^{inc} \right) \times \mathbf{h}^{inc}$, and $\tilde{\mathbf{e}}_s$ is the Fourier transform of the aperture basis mode for the electric field.

Interestingly, it follows from (15) that the modes of the open cavity can be determined by finding the frequencies for which

$$\text{Det} \left[\underline{\underline{Y}}^{cav} + \underline{\underline{Y}}^{rad} \right] = 0. \tag{16}$$

3.5. Hybrid formulation: ports and apertures

The use and verification of the RCM for apertures through quadratic (power) measurements requires the presence of antennas/ports inside the cavity. Therefore, it becomes natural to formulate a hybrid RCM including both the aperture admittance matrix and the port impedance matrix.

The RCM has been extended to account for the joint presence of electrically wide openings of arbitrary shape and localized ports. A schematic framework of such a situation is reported in Fig. 1. In that case, an input column vector $\underline{\phi}$ has been constructed that consists of the aperture basis mode voltages and port currents, and an output vector $\underline{\psi}$ consisting of the aperture basis mode currents and port voltages

$$\underline{\phi} = \begin{bmatrix} \underline{V}_A \\ \underline{I}_P \end{bmatrix} \tag{17}$$

and

$$\underline{\psi} = \begin{bmatrix} \underline{I}_A \\ \underline{V}_P \end{bmatrix} \tag{18}$$

where $\underline{V}_{A,P}$ are the aperture and port voltages, and $\underline{I}_{A,P}$ are the aperture and port currents. These are then related by a hybrid matrix $\underline{\underline{H}}$, $\underline{\psi} = \underline{\underline{H}} \cdot \underline{\phi}$, where

$$\underline{\underline{H}} = i \Im \left(\underline{\underline{U}} \right) + \left[\Re \left(\underline{\underline{U}} \right) \right]^{1/2} \cdot \underline{\underline{\xi}} \cdot \left[\Re \left(\underline{\underline{U}} \right) \right]^{1/2}. \tag{19}$$

Here, the matrix $\underline{\underline{U}}$ is block diagonal, viz.,

$$\underline{\underline{U}} = \begin{bmatrix} \underline{\underline{Y}}^{rad} & 0 \\ 0 & \underline{\underline{Z}}^{rad} \end{bmatrix}. \tag{20}$$

The dimension of $\underline{\underline{U}}$ is $(N_s + N_p) \times (N_s + N_p)$, where N_p is the number of port currents and N_s is the number of aperture basis mode voltages. The linear problem at hand is thus formulated in terms of matrices with relatively small dimensions,
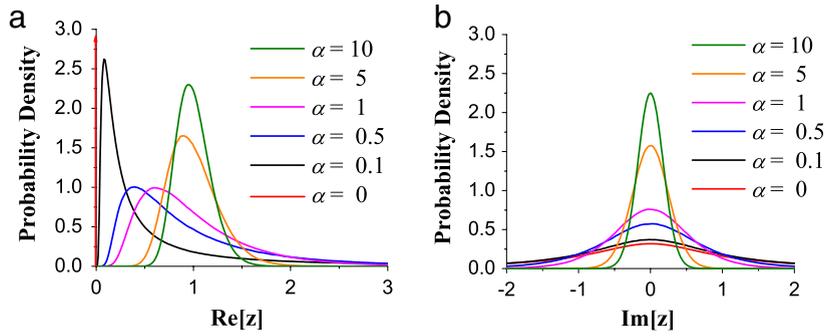
Fig. 3. Random matrix theory prediction for the statistical distributions of the real (a) and the imaginary (b) part of the universal fluctuation $z = \frac{z^{cav} - i\Im\{z^{rad}\}}{\Re\{z^{rad}\}}$ for various values of α.

typically given by the number of ports and aperture modes used to access the electromagnetic structure. Strictly speaking, the RCM formulation has facilitated a *model order reduction* [66] when compared to full-wave or other statistical models of cavity fields. Usually the superposition of plane-waves or modes requires the computation of the field at each point of the structure, thus producing very large matrices. In the different perspective of looking at ports, the available number of degrees of freedom (typically constituted by the number of excited modes of the cavity) is reduced to the number of port profiles and aperture basis functions.

4. Random coupling model in action

4.1. Numerical simulations

Once the system-specific properties of ports are predicted or measured separately under an $\alpha \rightarrow \infty$ (free-space) condition, Monte Carlo simulations of (4) allow for generating an ensemble of cavity impedances of the form (3) or, identically, of cavity admittances of the form (14). Ensembles of cavities have been generated by the application of the Monte Carlo method described in [40,41,30,93,94]. First of all, the universally fluctuating impedances (4) is recast in matrix form as

$$\underline{\underline{\xi}} = \frac{i}{\pi} \underline{\underline{\Phi}} \cdot \left[\underline{\underline{\lambda}} - i\alpha \underline{\underline{1}} \right]^{-1} \cdot \underline{\underline{\Phi}}^T. \tag{21}$$

The matrix $\underline{\underline{\Phi}}$ is a $M \times N$ coupling matrix with each element Φ_{ij} representing the coupling between the *i*th port profile/aperture mode ($1 \leq i \leq M$) and the *j*th mode of the cavity ($1 \leq j \leq N$). Each Φ_{ij} is an independent Gaussian-distributed random variable of zero mean and unit variance. The matrix $\underline{\underline{\Phi}}^T$ is the transpose of $\underline{\underline{\Phi}}$, and $\underline{\underline{1}}$ is a $N \times N$ identity matrix. The matrix $\underline{\underline{\lambda}}$ is an $N \times N$ diagonal matrix with a set of N random eigenvalues based on the GOE nearest-neighbor (Wigner) spacing distribution [44]. By repeating this procedure many times in order to give a sufficiently *large set of samples* of $\underline{\underline{Z}}$, the statistical description of the cavity is thus generated.

Conversely, starting from cavity measurements of the impedance, the universal fluctuation of the single port impedance can be calculated by normalization of experimental results, to compare to RMT predictions of the universal behavior [51,52]. Fig. 3 reports the distribution of the real (a) and the imaginary (b) part of the universal fluctuation parametrized as a function of the loss factor α. The loss parameter of the cavity at hand is predicted from the Weyl law on the basis of the volume of the cavity, its frequency of excitation ($\omega = kc$), and the electromagnetic losses. For a 3D enclosure it is found

$$\alpha = \frac{k^3 V}{2\pi^2 Q}, \tag{22}$$

where V is the cavity volume, and Q the average closed resonator quality factor. A proper number of realizations must be chosen to create adequate statistics close to the asymptotic behavior of the probability density function of $\Im\{Z\}$, which is Lorentzian in the lossless regime ($\alpha = 0$), and Gaussian in the high-loss regime ($\alpha \gg 1$), see Fig. 3.

The effect of increasing the loss parameter results in reducing the magnitude of fluctuation of impedance elements. It is to be noticed that for $\alpha = \infty$ we retrieve the case where ports/apertures radiate in free-space. In the limit of infinitesimal losses the impedance fluctuations become very strong: this is a situation that can occur in superconducting cavities [95], in low-loss optical systems, e.g., lasers [96], in quantum dots at low temperatures [97], in microwave cavities operated in the *non-Ericsson* (weak overlapping) regime [98,99], and in reverberation chambers/enclosures operated in the *undermoded* regime [71,100–105]. In the limit of high losses, the diagonal (off-diagonal) elements of $\underline{\underline{\xi}}$ become unit (zero) mean Gaussian random variables.
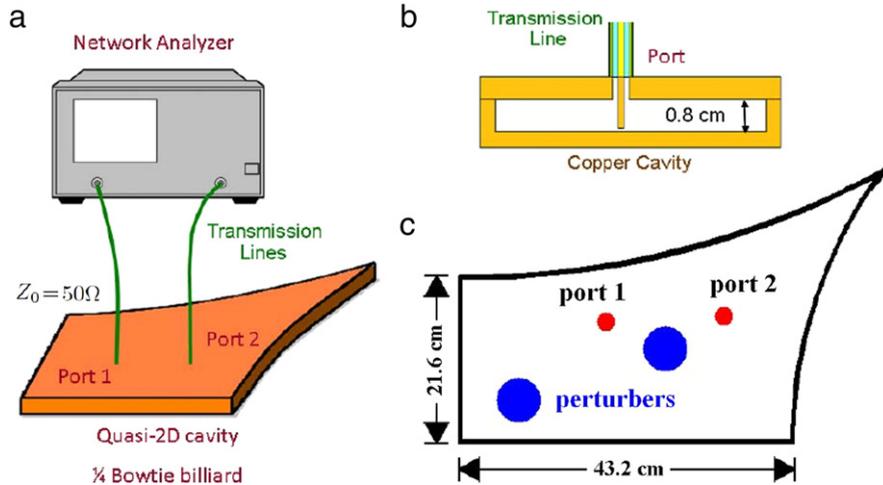
Fig. 4. Experimental set-up (a) and geometry (side view (b), top view (c)) of the "bowtie" billiard used for the measure of the cavity resistance and reactance to be compared with the RCM prediction.
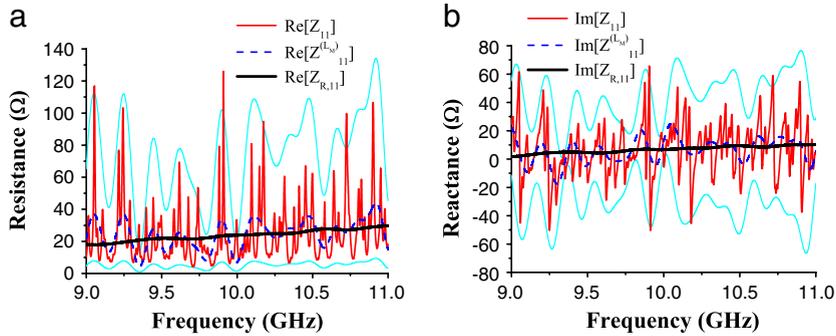

Fig. 5. Resistance $\Re\{Z_{11}\}$ (a) and reactance $\Im\{Z_{11}\}$ (b) of the measured port (input) impedance in a "bowtie" cavity. The solid red curves are measured data. The dashed blue curves are created by combining the short orbit effect and the radiation impedance (thick black curves). The solid cyan curves represent the 95% confidence interval boundaries on the impedance.

4.2. Comparison to experiments

Fig. 4 shows the experimental set-up (a) and geometry (side view (b), top view (c)) of the "bowtie" billiard adopted for the validation of the RCM. A calibrated network analyzer is used to measure the 2×2 scattering matrix $\underline{\underline{S}}$ of the billiard as a function of frequency and internal configuration of the perturbers. The impedance matrix is calculated as $\underline{\underline{Z}} = \underline{\underline{Z}}_0^{1/2}\left(\underline{\underline{I}} + \underline{\underline{S}}\right)\left(\underline{\underline{I}} - \underline{\underline{S}}\right)^{-1}\underline{\underline{Z}}_0^{1/2}$ where $\underline{\underline{Z}}_0$ is a diagonal matrix whose elements are the characteristic impedances of the transmission lines connected to the ports, which are 50 Ω in this case. Fig. 5 (red curves) reports a few experimental results for the frequency dependence of the real (a) and imaginary (b) two-port impedance matrix element Z_{11} measured at the coaxial port feeding a "bowtie" ray-chaotic cavity. A high frequency variability due to fluctuations that ride on top of several systematic trends can be noticed. The first systematic trend is shown as a black solid line and represents the measured radiation impedance of the port. The second systematic trend is shown as the thin dashed curves which are semi-numerical results that contain the radiation impedance (measured) and the effect of short (less than 200 cm-long) orbits. This should be compared to the characteristic dimension of this billiard, which is $\mathscr{L} = \sqrt{\mathscr{A}} \approx 34$ cm. Note that the short-orbit curve follows the major trend in the data, but does not describe the rapidly varying part of the impedance. In Fig. 5 (cyan curves) also show the 95% confidence interval boundaries. Here, the confidence interval indicates the reliability of the estimate of the impedance. Note that most of the measured impedance values fall within the 95% confidence interval. Rapid fluctuations in the impedance come from longer orbits. By removing all systematic effects up to an equivalent short orbit length of $\mathscr{L}_M = 200$ cm one can obtain a good correspondence between the RMT and experimental statistical properties of the universal random variable [57].

The question now arises: how far should the short-orbit calculation be carried? At short times only a few of the shortest orbits will contribute, whereas the number of orbits contributing to the impedance will grow exponentially as the time increases. The relevant time scale for terminating the short-orbit calculation is the Ehrenfest time. The Ehrenfest time is a
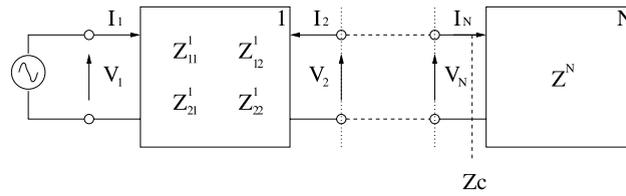
Fig. 6. Network model of a chain of coupled cavities: the first cavity is excited by a localized source (port 1), and the coupled field at the last cavity is picked up by a localized detector (port *N*). The cavity-to-cavity coupling can take place through either single-mode ports (transmission lines) or multimode ports (distributed ports or apertures).

time scale associated with the classical-to-quantum crossover [106], and it is the time when wave packets start to deviate from the motion of deterministic classical ray trajectories to fully-developed wave chaos [107]. Therefore, it is meaningless to compute the orbits whose lengths correspond to time scales much longer than the Ehrenfest time. For a microwave cavity, the Ehrenfest time can be calculated as

$$t_E = \frac{1}{h} \ln \left(\frac{\mathcal{L}}{\lambda} \right),$$ (23)

where h is the largest Lyapunov exponent of the classical ray dynamics in the cavity, $\mathcal{L}$ is the characteristic dimension of the cavity, and λ is the wavelength of the probing waves. The Ehrenfest times of the bowtie cavity has been estimated to be 3.2 ns (at $f = 10$ GHz), which corresponds to a length of 94 cm in free space. Here our treatment of short orbits up to a length of 200 cm is justified.

5. Interconnection of cavities

The RCM has been pushed further ahead to address the interconnection of complicated systems. Hence, the scenario of a linear chain of cavities has been investigated [65].

The analyzed physical framework consists of N interconnected two-port cavities, as shown in Fig. 6. A fundamental quantity of interest for this analysis is the input impedance of the chain. This can be found in an iterated manner starting at the last cavity, where $Z_{in}^{(N)} = Z_{11}^{(N)}$, to the first cavity, to find $Z_{in}^{(1)}$

$$Z_{in}^{(n)} = Z_{11}^{(n)} - \frac{\left(Z_{12}^{(n)} \right)^2}{\left(Z_{22}^{(n)} + Z_{in}^{(n+1)} \right)}.$$ (24)

The concept of *trans-impedance* has been adopted as a baseline to analyze and quantify the amount of signal coupled between two or more arbitrary elements (subsystems) of the chain. In particular, for the n-th cavity, the voltage at the first port of the $n + 1$-st cavity $V_1^{(n+1)}$ is related to the current exciting the first port of the n-th cavity $I_1^{(n)}$ as

$$Z_T^{(n)} = \frac{V_1^{(n+1)}}{I_1^{(n)}} = \frac{Z_{in}^{(n+1)} Z_{21}^{(n)}}{Z_{22}^{(n)} + Z_{in}^{(n+1)}}.$$ (25)

Consequently, the ratio of power entering the N-th cavity to that entering the first cavity can be expressed as a product, viz.,

$$R_N \equiv \frac{P_{in}^{(N)}}{P_{in}^{(1)}},$$ (26)

where each impedance involved in (25) is expressed by the RCM.

The case of statistically identical cavities having moderate/high losses $\alpha_1 = \alpha_2 = \cdots = \alpha_N = \alpha > 1$, deserves special attention. Correspondingly, the weak fluctuation approximation can be employed leading to a simplified expression of (25). More precisely, in the high-loss regime, $Z_{in}^{(n)} \approx Z_{11}^{(n)}$, and fluctuating impedances can be tackled with first-order perturbation theory. This procedure results in a simplification for the denominator of (25), and leads to an expression for the coupled power ratio R_N that factorizes

$$R_N(\alpha) \approx \prod_{n=1}^{N-1} x^{(n)} \frac{t^{(n,n+1)}}{2\pi\alpha},$$ (27)

where $x^{(n)}$ are exponentially distributed random variables

$$f_X(x) = \exp(-x).$$ (28)
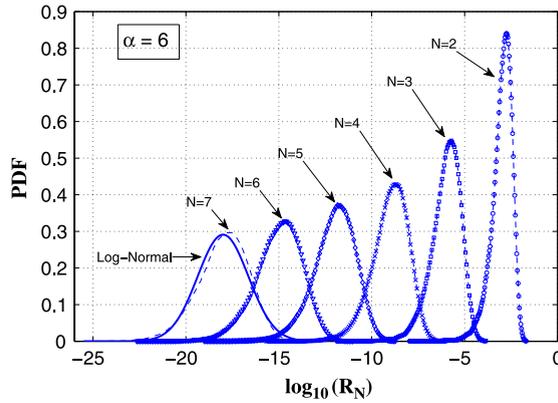
Fig. 7. Probability density function of power ratios R_N ($\alpha = 6$) $\equiv \frac{P_{in}^{(N)}}{P_{in}^{(1)}}$ for chains of up to seven cavities: the high-loss regime is assumed for all the (statistically identical) cavities in the chain.

The transmission factors in (27) are given by

$$t^{(n,n+1)} = \frac{R_{22,rad}^{(n)} R_{11,rad}^{(n+1)}}{\left| Z_{22,rad}^{(n)} + Z_{11,rad}^{(n+1)} \right|^2}, \tag{29}$$

modeling the coupling between the n-th and $n + 1$-st cavity, and the loss factor is given by (22). In [65], the Monte Carlo method described in Section 4 has been used to generate ensembles of impedance matrices and compute the coupling in chains of cavities. Basically, the impedance matrix for each single cavity has been generated, and used in the theoretical expressions (3) and (21). Then, the power ratio has been evaluated for sequences of cavity chains of different length. For these studies, the cavities were assumed to be statistically identical. The PDFs of the logarithm of the power ratio for the case $\alpha = 6$ is shown in Fig. 7. The high loss case (Fig. 7) is well approximated by the analytic formulas (27)–(29). The distribution approaches log-normal as the number of cavities becomes large. This is evident from the comparison of the 7-cavity chain with a best-fit log-normal distribution. This behavior is expected since according to (27) and (28) the power ratio becomes a product of N independent and identically distributed random variables, and thus, as N becomes large the logarithm of the power ratio will be normally distributed. In the lossless case, a phenomenon similar to Anderson localization has been observed with respect to the number of chain elements by adopting a cascaded RCM in a chaotic dynamics perspective [65]. In the context of reverberation chambers, the modeling of coupled cavities is useful to evaluate the shielding effectiveness of metallic structures and materials [108].

### 5.1. Connection with acoustics and vibrations

It turns out that the flow of electromagnetic energy can be expressed in a similar way to that used to model the flow of vibrational wave energy. The global system is divided into complex subsystems interconnected with each other through simple deterministic structures. In particular, [13] applied a "thermodynamical" approach to arrive at a statistical model of energy exchange between two parts (subsystems) of the system, namely statistical energy analysis (SEA). Specifically, by using energy *equipartition* arguments, the average power passing from subsystem i to subsystem j (P_{ij}) can be expressed as [11, Eq. (92)]

$$P_{ij} = \omega \bar{d}_i \eta_{ij} \left(\frac{E_i}{\bar{d}_i} - \frac{E_j}{\bar{d}_j} \right), \tag{30}$$

where ω is the mean frequency of the source, η_{ij} is the coupling loss factor, $\bar{d}_{(\cdot)}$ is the mean density of eigenfrequencies (modes) of the uncoupled subsystems, and $E_{(\cdot)}$ is the energy stored in each subsystem. In a similar way, by recalling the average power ratio (27), it is worth noticing that the difference between the power entering two arbitrary elements of the chain can be written in the very general form

$$P_{ij} = \frac{P_i T^{(i,j)}}{2\pi \alpha^{(i)}} - \frac{P_j T^{(i,j)}}{2\pi \alpha^{(j)}}, \tag{31}$$

valid for an arbitrary chain section of two elements, In (31), P_i is the input power entering cavity i, and P_j is the input power entering cavity j. In equilibrium, the net power exchange between the to subsystems is established by the power dissipated in each cavity, and by the fraction of power leaking through the small (deterministic) port. The scheme of the physical
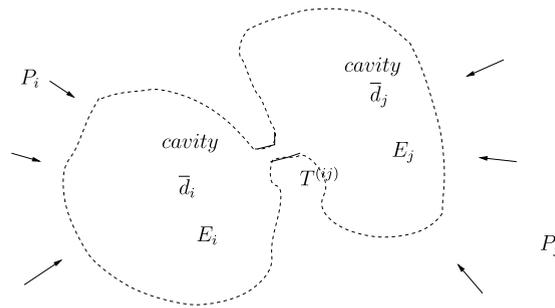
Fig. 8. Arbitrary section of a chain: two cavities are excited by different input powers and they are weakly coupled. This simplified framework has been used to calculate the net power exchanged by the two cavities. A similar attack is adopted by the statistical energy analysis (SEA) approach in acoustics.

framework analyzed to derive (31) is reported in Fig. 8. By using (5) the loss factor $\alpha^{(\cdot)}$, and by assuming

$$\frac{P_i}{P_d^{(i)}} \approx \frac{P_j}{P_d^{(j)}} = L, \tag{32}$$

where L is a dissipation factor of the subsystem since $P_d^{(\cdot)}$ is the dissipated power within each cavity, it is found that

$$P_{ij} \approx \omega \frac{L}{2\pi} T^{(ij)} \left(\frac{E_i}{\bar{d}_i} - \frac{E_j}{\bar{d}_j} \right), \tag{33}$$

where a coupling loss factor $\eta_{ij} = T^{(ij)}/2\pi$ is recognized, and

$$\bar{d}_{(\cdot)} = \frac{k^2}{\Delta k_{(\cdot)}^2}, \tag{34}$$

is the mean (mode) density of each subsystem. The assumption in (32) is related to the equipartition of energy. This results in (33) are formally similar to (30) even in the case of autonomous (sub)systems coupled by an electrically short transmission line. Interestingly, in deriving the terms of (33), a weak coupling argument has been used [65] that is identical to the one typically used in SEA [109]. Methods based on SEA have been recently integrated with the finite element method (FEM) to tackle very complex vibro-acoustic scenarios [110]. In general, the application of techniques developed in acoustics and vibrations to electromagnetic problems constitute a modern and active field of research [2].

6. Conclusion and future perspective

The general "dressed" impedance obtained in formulating the RCM for ports and apertures radiating inside complex electromagnetic cavities has been reviewed. This statistical model accounts for distributed losses, and is able to describe short orbit deviations, as well as other deterministic (system specific) deviations, from the full random matrix description. Numerical and experimental results validate the "dressing" of a universal fluctuating impedance matrix (dependent on a single loss parameter) with the radiation impedance matrix (modeling the coupling properties of ports). The recent extension to 3D open cavities is described in terms of the admittance matrix by solving the vector electromagnetic aperture problem, also accounting for the aperture irradiation with an external plane-wave. A generalization of the RCM to the scenario of interconnected cavities for weak coupling conditions is presented, and the distribution of the power flowing through such a chain discussed for an increasing number of cavities. The analogy with Statistical Energy Analysis used in vibro-acoustics is pointed out by formulating a new model for the power exchanged by two wave chaotic cavities excited by different input powers.

The RCM provides a unique framework to study the very complicated scenario of circuits operating in complex cavities with arbitrary losses. The ability to include short orbit effects is of fundamental interest to explain and exploit unstirred components in reverberation chambers [71,111]. The interconnected cavities formulation offers a chance to include the RCM in codes already employed in acoustics and vibrations to perform statistical energy analysis of electromagnetic waves. Rich fading scenarios in structured wireless channels can also be tackled by the joint application of RCM for apertures and interconnected cavities.

Acknowledgments

References

[1] D. Hill, Electromagnetic Fields in Cavities: Deterministic and Statistical Theories, in: IEEE Press Series on Electromagnetic Wave Theory, Wiley, 2009.
[2] R. Langley, A reciprocity approach for computing the response of wiring systems to diffuse electromagnetic fields, IEEE Trans. Electromagn. Compat. 52 (4) (2010) 1041–1055.
[3] E.P. Wigner, L. Eisenbud, Higher angular momenta and long range interaction in resonance reactions, Phys. Rev. 72 (1947) 29.
[4] G.E. Mitchell, A. Richter, H.A. Weidenmuller, Random matrices and chaos in nuclear physics: nuclear reactions, Rev. Modern Phys. 82 (2010) 2845.
[5] F. Beck, C. Dembowski, A. Heine, A. Richter, R-matrix theory of driven electromagnetic cavities, Phys. Rev. E 67 (2003) 066208.
[6] T. Guhr, A. Müller-Groeling, H.A. Weidenmüller, Random-matrix theories in quantum physics: common concepts, Phys. Rep. 299 (1998) 189.
[7] H.A. Weidenmüller, G.E. Mitchell, Random matrices and chaos in nuclear physics: nuclear structure, Rev. Modern Phys. 81 (2009) 539–589.
[8] C.W.J. Beenakker, Random-matrix theory of quantum transport, Rev. Modern Phys. 69 (1997) 731.
[9] Y. Alhassid, The statistical theory of quantum dots, Rev. Modern Phys. 72 (2000) 895–968.
[10] L. Couchman, E. Ott, T.M. Antonsen, Quantum chaos in systems with ray splitting, Phys. Rev. A 46 (1992) 6193–6210.
[11] G. Tanner, N. Sondergaard, Wave chaos in acoustics and elasticity, J. Phys. A 40 (50) R443–R509.
[12] M. Wright, R. Weaver, New Directions in Linear Acoustics and Vibration: Quantum Chaos, Random Matrix Theory and Complexity, Cambridge University Press, 2010.
[13] R. Lyon, Statistical Energy Analysis of Dynamical Systems: Theory and Applications, Mit Press, 2003.
[14] D. Maksimov, G. Tanner, A hybrid approach for predicting the distribution of vibro-acoustic energy in complex built-up structures, J. Acoust. Soc. Am. 130 (2011) 1337–1347.
[15] U. Kuhl, M. Martínez-Mares, R.A. Méndez-Sánchez, H.J. Stöckmann, Direct processes in chaotic microwave cavities in the presence of absorption, Phys. Rev. Lett. 94 (2005) 144101.
[16] R.A. Méndez-Sánchez, U. Kuhl, M. Barth, C.H. Lewenkopf, H.-J. Stöckmann, Distribution of reflection coefficients in absorbing chaotic microwave cavities, Phys. Rev. Lett. 91 (2003) 174102.
[17] H.-J. Stöckmann, J. Stein, Quantum chaos in billiards studied by microwave absorption, Phys. Rev. Lett. 64 (1990) 2215.
[18] E. Doron, U. Smilansky, A. Frenkel, Experimental demonstration of chaotic scattering of microwaves, Phys. Rev. Lett. 65 (1990) 3072.
[19] S. Sridhar, Experimental observation of scarred eigenfunctions of chaotic microwave cavities, Phys. Rev. Lett. 67 (1991) 785–788.
[20] H.-D. Gräf, H.L. Harney, H. Lengeler, C.H. Lewenkopf, C. Rangacharyulu, A. Richter, P. Schardt, H.A. Weidenmüller, Distribution of eigenmodes in a superconducting stadium billiard with chaotic dynamics, Phys. Rev. Lett. 69 (1992) 1296–1299.
[21] C. Poli, D.V. Savin, O. Legrand, F. Mortessagne, Statistics of resonance states in open chaotic systems: a perturbative approach, Phys. Rev. E 80 (2009) 046203.
[22] H.-J. Stöckmann, E. Persson, Y.-H. Kim, M. Barth, U. Kuhl, I. Rotter, Effective Hamiltonian for a microwave billiard with attached waveguide, Phys. Rev. E 65 (2002) 066211.
[23] D.V. Savin, Y.V. Fyodorov, H.-J. Sommers, Reducing nonideal to ideal coupling in random matrix description of chaotic scattering: application to the time-delay problem, Phys. Rev. E 63 (2001) 035202(R).
[24] Y.V. Fyodorov, D.V. Savin, Statistics of impedance, local density of states, and reflection in quantum chaotic systems with absorption, JETP Lett. 80 (2004) 725.
[25] D.V. Savin, H.-J. Sommers, Distribution of reflection eigenvalues in many-channel chaotic cavities with absorption, Phys. Rev. E 69 (2004) 035201(R).
[26] Y.V. Fyodorov, D.V. Savin, H.-J. Sommers, Scattering, reflection and impedance of waves in chaotic and disordered systems with absorption, J. Phys. A: Math. Gen. 38 (2005) 10731.
[27] D.V. Savin, H.-J. Sommers, Y.V. Fyodorov, Universal statistics of the local Green's function in wave chaotic systems with absorption, JETP Lett. 82 (2005) 544.
[28] S.W. McDonald, A.N. Kaufman, Spectrum and eigenfunctions for a Hamiltonian with stochastic trajectories, Phys. Rev. Lett. 42 (1979) 1189.
[29] H.J. Stöckmann, Quantum Chaos: An Introduction, Cambridge University Press, Cambridge, England, 1999.
[30] S. Hemmady, T.M. Antonsen, E. Ott, S.M. Anlage, Statistical prediction and measurement of induced voltages on components within complicated enclosures: a wave-chaotic approach, IEEE Trans. Electromagn. Compat. 54 (2012) 758–771.
[31] P.W. Brouwer, Generalized circular ensemble of scattering matrices for a chaotic cavity with nonideal leads, Phys. Rev. B 51 (1995) 16878.
[32] N. Taniguchi, V.N. Prigodin, Distribution of the absorption by chaotic states in quantum dots, Phys. Rev. B 54 (1996) R14305.
[33] Y.V. Fyodorov, H.J. Sommers, Statistics of resonance poles, phase shifts and time delays in quantum chaotic scattering: Random matrix approach for systems with broken time-reversal invariance, J. Math. Phys. 38 (1997) 1918.
[34] F. Haake, Quantum Signatures of Chaos, second ed., Springer, Berlin, 2000.
[35] Y. Alhassid, The statistical theory of quantum dots, Rev. Modern Phys. 75 (2000) 895.
[36] K. Richter, M. Sieber, Semiclassical theory of chaotic quantum transport, Phys. Rev. Lett. 89 (2002) 206801.
[37] P.A. Mello, N. Kumar, Quantum Transport in Mesoscopic Systems, Oxford University Press, New York, 2004.
[38] S. Müller, S. Heusler, P. Braun, F. Haake, Semiclassical approach to chaotic quantum transport, New J. Phys. 9 (2007) 12.
[39] X. Zheng, Statistics of impedance and scattering matrices in microwave chaotic cavities: the random coupling model, Ph.D. Thesis, University of Maryland, College Park, 2005, http://hdl.handle.net/1903/2920.
[40] X. Zheng, T.M. Antonsen, E. Ott, Statistics of impedance and scattering matrices in chaotic microwave cavities: Single channel case, Electromagnetics 26 (2006) 3.
[41] X. Zheng, T.M. Antonsen, E. Ott, Statistics of impedance and scattering matrices of chaotic microwave cavities with multiple ports, Electromagnetics 26 (2006) 37.
[42] R. Holland, R.S. John, Statistical Electromagnetics, Taylor and Francis, 1999.
[43] F. Schwabl, W. Brewer, Statistical Mechanics, in: Advanced Texts in Physics, Springer, 2006.
[44] E. Wigner, Random matrices in physics, SIAM Rev. 9 (1) (1967) 1–23.
[45] M.V. Berry, Regular and irregular semiclassical wavefunctions, J. Phys. A 10 (1977) 2083.
[46] J.G. Kostas, B. Boverie, Statistical model for a mode-stirred chamber, IEEE Trans. Electromagn. Compat. 33 (1991) 366.
[47] L. Arnaut, Statistics of the quality factor of a rectangular reverberation chamber, IEEE Trans. Electromagn. Compat. 45 (1) (2003) 61–76.
[48] H. Ishio, J. Burgdörfer, Quantum conductance fluctuations and classical short-path dynamics, Phys. Rev. B 51 (1995) 2013.
[49] H.U. Baranger, P.A. Mello, Short paths and information theory in quantum chaotic scattering: transport through quantum dots, Europhys. Lett. 33 (1996) 465.
[50] J.A. Hart, T.M. Antonsen, E. Ott, Effect of short ray trajectories on the scattering statistics of wave chaotic systems, Phys. Rev. E 80 (2009) 041109.
[51] S. Hemmady, X. Zheng, E. Ott, T.M. Antonsen, S.M. Anlage, Universal impedance fluctuations in wave chaotic systems, Phys. Rev. Lett. 94 (2005) 014102.
[52] S. Hemmady, X. Zheng, T.M. Antonsen, E. Ott, S.M. Anlage, Universal statistics of the scattering coefficient of chaotic microwave cavities, Phys. Rev. E 71 (2005) 056215.
[53] S. Hemmady, X. Zheng, T.M. Antonsen, E. Ott, S.M. Anlage, Universal properties of two-port scattering, impedance, and admittance matrices of wave-chaotic systems, Phys. Rev. E 74 (2006) 036213.
[54] S. Hemmady, X. Zheng, T.M. Antonsen, E. Ott, S.M. Anlage, Aspects of the scattering and impedance properties of chaotic microwave cavities, Acta Phys. Polon. A 109 (2006) 65.
[55] X. Zheng, S. Hemmady, T.M. Antonsen, S.M. Anlage, E. Ott, Characterization of fluctuations of impedance and scattering matrices in wave chaotic scattering, Phys. Rev. E 73 (2006) 046208.

[56] J.-H. Yeh, J.A. Hart, E. Bradshaw, T.M. Antonsen, E. Ott, S.M. Anlage, Universal and nonuniversal properties of wave-chaotic scattering systems, Phys. Rev. E 81 (2010) 025201(R).
[57] J.-H. Yeh, J.A. Hart, E. Bradshaw, T.M. Antonsen, E. Ott, S.M. Anlage, Experimental examination of the effect of short ray trajectories in two-port wave-chaotic scattering systems, Phys. Rev. E 82 (2010) 041114.
[58] J.-H. Yeh, T.M. Antonsen, E. Ott, S.M. Anlage, First-principles model of time-dependent variations in transmission through a fluctuating scattering environment, Phys. Rev. E 85 (2012) 015202 (Rapid Communications).
[59] J.-H. Yeh, T.M. Antonsen, E. Ott, S.M. Anlage, Fading statistics in communications — a random matrix approach, Acta Phys. Polon. A 120 (2012) A-85.
[60] T.M. Antonsen, G. Gradoni, S. Anlage, E. Ott, Statistical characterization of complex enclosures with distributed ports, in: Proceedings of the IEEE International Symposium on EMC, Long Beach, CA, USA, 2011, pp. 220–225.
[61] G. Gradoni, T. Antonsen, S. Anlage, E. Ott, External radiation of complex cavities described by the random coupling model, in: 2012 International Conference on Electromagnetics in Advanced Applications, ICEAA, 2012, pp. 357–358.
[62] G. Gradoni, T. Antonsen, S. Anlage, E. Ott, Coupling of external radiation to circuitry inside complex em environments, in: 2012 International Conference on Electromagnetics in Advanced Applications, ICEAA, 2012, pp. 1233–1234.
[63] G. Gradoni, T.M. Antonsen, S. Anlage, E. Ott, Theoretical analysis of apertures radiating inside wave chaotic cavities, in: Proceedings of the EMC Europe, Rome, Italy, 2012, pp. 1–6.
[64] M.-J. Lee, T.M. Antonsen, E. Ott, Statistical model of short wavelength transport through cavities with coexisting chaotic and regular ray trajectories, Phys. Rev. E 87 (2013) 062906.
[65] G. Gradoni, T.M. Antonsen, E. Ott, Impedance and power fluctuations in linear chains of coupled wave chaotic cavities, Phys. Rev. E 86 (2012) 046204.
[66] L.B. Felsen, M. Mongiardo, P. Russer, Electromagnetic Field Computation by Network Methods, Springer, 2007.
[67] M.L. Mehta, Random Matrices, second ed., Academic Press, Boston, 1991.
[68] M. Born, E. Wolf, Principles of Optics: Electromagnetic Theory of Propagation, Interference and Diffraction of Light, Cambridge University Press, 1999.
[69] J. Barthélemy, O. Legrand, F. Mortessagne, Complete S matrix in a microwave cavity at room temperature, Phys. Rev. E 71 (2005) 016205.
[70] C. Poli, O. Legrand, F. Mortessagne, Statistics of resonance states in a weakly open chaotic cavity with continuously distributed losses, Phys. Rev. E 82 (2010) 055201.
[71] L. Arnaut, Operation of electromagnetic reverberation chambers with wave diffractors at relatively low frequencies, IEEE Trans. Electromagn. Compat. 43 (4) (2001) 637–653.
[72] P.W. Brouwer, C.W.J. Beenakker, Voltage-probe and imaginary-potential models for dephasing in a chaotic quantum dot, Phys. Rev. B 55 (1997) 4695.
[73] R. Schäfer, H.-J. Stöckmann, T. Gorin, T.H. Seligman, Experimental verification of fidelity decay: from perturbative to Fermi golden rule regime, Phys. Rev. Lett. 95 (2005) 184102.
[74] B. Köber, U. Kuhl, H.-J. Stöckmann, A. Goussev, K. Richter, Fidelity decay for local perturbations: microwave evidence for oscillating decay exponents, Phys. Rev. E 83 (2011) 016214.
[75] G. Gradoni, V. Primiani, F. Moglie, Reverberation chamber as a multivariate process: FDTD evaluation of correlation matrix and independent positions, Prog. Electromagn. Res. 133 (2) (2013) 217–234.
[76] R.E. Prange, Resurgence in quasi-classical scattering, J. Phys. A: Math. Gen. 38 (2005) 10703.
[77] E.N. Bulgakov, V.A. Gopar, P.A. Mello, I. Rotter, Statistical study of the conductance and shot noise in open quantum-chaotic cavities: Contribution from whispering gallery modes, Phys. Rev. B 73 (2006) 155302.
[78] IEC SC77B-CISPR/A JWG REV, IEC 61000-4-21: Electromagnetic Compatibility (EMC) – Part 4-21: Testing and Measurement Techniques – Reverberation chamber test methods (International Electrotechnical Commission, Geneva, Swiitzerland, August 2003).
[79] V. Primiani, F. Moglie, V. Paolella, Numerical and experimental investigation of unstirred frequencies in reverberation chambers, in: IEEE International Symposium on Electromagnetic Compatibility, 2009. EMC 2009, 2009, pp. 177–181.
[80] V.M. Primiani, F. Moglie, Numerical simulation of los and nlos conditions for an antenna inside a reverberation chamber, J. Electromagn. Waves Appl. 24 (17-18) (2010) 2319–2331.
[81] R. Pirkl, J. Ladbury, K. Remley, The reverberation chamber's unstirred field: a validation of the image theory interpretation, in: 2011 IEEE International Symposium on Electromagnetic Compatibility, EMC, 2011, pp. 670–675.
[82] P.A. Mello, P. Peveyra, T.H. Seligman, Information theory and statistical nuclear reactions. I. General theory and applications to few-channel problems, Ann. Physics 161 (1985) 254.
[83] R.E. Prange, E. Ott, J.T.M. Antonsen, B. Georgeot, R. Blümel, Smoothed density of states for problems with ray splitting, Phys. Rev. E 53 (1996) 207.
[84] E.B. Bogomolny, Semiclassical quantization of multidimensional systems, Nonlinearity 5 (1992) 805.
[85] J.D. Urbina, K. Richter, Statistical description of eigenfunctions in chaotic and weakly disordered systems beyond universality, Phys. Rev. Lett. 97 (2006) 214101.
[86] T. Kottos, U. Smilansky, Quantum graphs: a simple model for chaotic scattering, J. Phys. A: Math. Gen. 36 (2003) 3501.
[87] J. Stein, H.-J. Stöckmann, Experimental determination of billiard wave functions, Phys. Rev. Lett. 68 (1992) 2867.
[88] R. Harrington, Resonant behavior of a small aperture backed by a conducting body, IEEE Trans. Antennas and Propagation 30 (2) (1982) 205–212.
[89] H.A. Bethe, Theory of diffraction by small holes, Phys. Rev. 66 (7) (1944) 163–182.
[90] R.F. Harrington, J.R. Mautz, A generalized network formulation for aperture problems, IEEE Trans. Antennas and Propagation 24 (6) (1976) 870–873.
[91] C. Bunting, S.-P. Yu, Field penetration in a rectangular box using numerical techniques: an effort to obtain statistical shielding effectiveness, IEEE Trans. Electromagn. Compat. 46 (2) (2004) 160–168.
[92] R.F. Harrington, Time-Harmonic Electromagnetic Fields, first ed., McGraw-Hill Book Company, New York, 1961.
[93] S. Hemmady, A wave-chaotic approach to predicting and measuring electromagnetic field quantities in complicated enclosures, Ph.D. Thesis, University of Maryland, College Park, 2006. http://hdl.handle.net/1903/3979.
[94] J.-H. Yeh, Wave chaotic experiments and models for complicated wave scattering systems, Ph.D. Thesis, University of Maryland, College Park, 2013. http://hdl.handle.net/1903/14651.
[95] H. Alt, A. Bäcker, C. Dembowski, H.-D. Gräf, R. Hofferbert, H. Rehfeld, A. Richter, Mode fluctuation distribution for spectra of superconducting microwave billiards, Phys. Rev. E 58 (1998) 1737–1742.
[96] H.E. Türeci, A.D. Stone, B. Collier, Self-consistent multimode lasing theory for complex or random lasing media, Phys. Rev. A 74 (2006) 043822.
[97] A.G. Huibers, S.R. Patel, C.M. Marcus, P.W. Brouwer, C.I. Duruöz, J.S. Harris, Distributions of the conductance and its parametric derivatives in quantum dots, Phys. Rev. Lett. 81 (1998) 1917–1920.
[98] B. Dietz, T. Friedrich, H.L. Harney, M. Miski-Oglu, A. Richter, F. Schäfer, H.A. Weidenmüller, Chaotic scattering in the regime of weakly overlapping resonances, Phys. Rev. E 78 (2008) 055204.
[99] B. Dietz, T. Friedrich, H.L. Harney, M. Miski-Oglu, A. Richter, F. Schäfer, J. Verbaarschot, H.A. Weidenmüller, Induced violation of time-reversal invariance in the regime of weakly overlapping resonances, Phys. Rev. Lett. 103 (2009) 064101.
[100] L. Warne, K. Lee, H. Hudson, W. Johnson, R. Jorgenson, S. Stronach, Statistical properties of linear antenna impedance in an electrically large cavity, IEEE Transactions on Antennas and Propagation 51 (5) (2003) 978–992.
[101] G. Orjubin, E. Richalot, S. Mengue, O. Picon, Statistical model of an undermoded reverberation chamber, IEEE Trans. Electromagn. Compat. 48 (1) (2006) 248–251.
[102] C. Holloway, D. Hill, M. Sandroni, J. Ladbury, J. Coder, G. Koepke, A. Marvin, Y. He, Use of reverberation chambers to determine the shielding effectiveness of physically small, electrically large enclosures and cavities, IEEE Trans. Electromagn. Compat. 50 (4) (2008) 770–782.
[103] D. Fedeli, G. Gradoni, V. Primiani, F. Moglie, Accurate analysis of reverberation field penetration into an equipment-level enclosure, IEEE Trans. Electromagn. Compat. 51 (2) (2009) 170–180.

[104] G. Gradoni, L. Arnaut, Higher order statistical characterization of received power fluctuations for partially coherent random fields, IEEE Trans. Electromagn. Compat. 51 (3) (2009) 583–591.
[105] L. Arnaut, G. Gradoni, On distributions of fields and power in undermoded mode-stirred reverberation chambers, in: General Assembly and Scientific Symposium, 2011 XXXth URSI, 2011, pp. 1–4.
[106] I.L. Aleiner, A.I. Larkin, Divergence of classical trajectories and weak localization, Phys. Rev. B 54 (1996) 14423–14444.
[107] H. Schomerus, P. Jacquod, Quantum-to-classical correspondence in open chaotic systems, J. Phys. A: Math. Gen. 38 (49) (2005) 10663.
[108] A. Cicchi, L. D'Ignazi, G. Gradoni, F. Moglie, A.P. Pastore, V.M. Primiani, Automatic procedure for shielding effectiveness measurements by means of a nested reverberation chamber, in: EMC Europe Workshop, Paris, France, 2007.
[109] R. Langley, A derivation of the coupling loss factors used in statistical energy analysis, J. Sound Vib. 141 (2) (1990) 207–219.
[110] D. Chappell, G. Tanner, Solving the stationary Liouville equation via a boundary element method, J. Comput. Phys. 234 (0) (2013) 487–498.
[111] G. Tait, C. Hager, M. Slocum, M. Hatfield, On measuring shielding effectiveness of sparsely moded enclosures in a reverberation chamber, IEEE Transactions on Electromagn. Compat. 55 (2) (2013) 231–240.